NASA TECHNICAL MEMORANDUM

NASA TM X-3053

NASA TM X-3053

FLIGHT REYNOLDS NUMBER EFFECTS ON A CONTOURED BOATTAIL NOZZLE AT SUBSONIC SPEEDS

by Roger Chamberlin

Lewis Research Center

Cleveland, Ohio 44135

NATIONAL AERONAUTICS AND SPACE ADMINISTRATION • WASHINGTON, D. C. • MAY 1974

1. Report No.	2. Government Accession No.	3. Recipient's Catalog No.
NASA TM X-3053		

4. Title and Subtitle	5. Report Date
FLIGHT REYNOLDS NUMBER EFFECTS ON A CONTOURED BOATTAIL NOZZLE AT SUBSONIC SPEEDS	MAY 1974
	6. Performing Organization Code

7. Author(s)	8. Performing Organization Report No.
Roger Chamberlin	E-7818
	10. Work Unit No. 501-24
9. Performing Organization Name and Address Lewis Research Center National Aeronautics and Space Administration Cleveland, Ohio 44135	11. Contract or Grant No.
	13. Type of Report and Period Covered Technical Memorandum
12. Sponsoring Agency Name and Address National Aeronautics and Space Administration Washington, D.C. 20546	14. Sponsoring Agency Code

15. Supplementary Notes

16. Abstract

A contoured boattail nozzle typical of those used on a twin-engine fighter was tested on an underwing nacelle mounted on an F-106B aircraft. The gas generator was a J85-GE-13 turbojet engine. The effects of Reynolds number, Mach number, and angle of attack on boattail drag and boattail pressure profiles were investigated. Increasing Reynolds number caused a slight reduction in boattail drag at both Mach 0.7 and 0.9. The nozzle had relatively low boattail drag even though the flow was separated over a large portion of the boattail.

17. Key Words (Suggested by Author(s))	18. Distribution Statement
Boattail; Flow separation; Reynolds number effects; Flight test; Propulsion system; Transonic	Unclassified - unlimited Category 01

19. Security Classif. (of this report)	20. Security Classif. (of this page)	21. No. of Pages	22. Price*
Unclassified	Unclassified	24	$3.00

* For sale by the National Technical Information Service, Springfield, Virginia 22151

FLIGHT REYNOLDS NUMBER EFFECTS ON A CONTOURED BOATTAIL NOZZLE AT SUBSONIC SPEEDS

by Roger Chamberlin

Lewis Research Center

SUMMARY

A contoured boattail nozzle typical of those used on a twin-engine fighter was tested on an underwing nacelle mounted on an F-106B aircraft. The gas generator was a J85-GE-13 turbojet engine. The effects of Reynolds number, Mach number, and angle of attack on boattail drag and boattail pressure profiles were investigated.

Increasing Reynolds number caused a slight reduction in boattail drag at both Mach numbers of 0.7 and 0.9. This effect was more pronounced at Mach 0.7 and at the lower Reynolds numbers at Mach 0.9. The relatively small change in drag was associated with the small change in the extent of the separated region over the Reynolds number range. The boattail drag levels of this nozzle were relatively low, even though the flow over a sizable portion of the boattail was separated. The geometry of this nozzle caused the flow to recompress to high pressures before it separated, so that the separated region had high pressure and little or no drag.

INTRODUCTION

The Lewis Research Center is conducting a flight program to investigate the installed performance of various exhaust nozzles on a turbojet engine (refs. 1 to 4). The powerplant installation being studied is a nacelle mounted under the aft portion of the wing of a modified F-106B aircraft (fig. 1) with the exhaust nozzle just downstream of the wing trailing edge. Various nozzles designed for supersonic cruise have been tested. Some of the more recent studies have concerned boattail nozzles designed for use on afterburning turbofan engines on aircraft that would have supersonic dash capability, but which cruise subsonically (refs. 5 and 6). The program described in this report was a test of a boattail typical of those used on a twin-engine fighter aircraft. The nozzle was fixed with the boattail in the closed or subsonic cruise configuration. The purpose of

this program was to determine the effects of Reynolds number on the boattail drag and pressure distribution of this particular boattail geometry. The geometry was such that there was very little curvature initially and most of the turning occurred on the rear half of the nozzle length. Because of the gradual turning on the upstream portion and the necessity of keeping the nozzle reasonably short, high boattail angles resulted on the downstream portion of the boattail. This geometry also resulted in 80 percent of the projected boattail area being on the downstream half of the nozzle length.

Other geometries of rounded shoulder boattails have been tested previously for Reynolds number effects (refs. 5 and 6). In the flight range of Reynolds numbers the previous boattails have all shown a reduction in boattail drag with increasing Reynolds number. Some of the geometries experienced only a small effect, while on others the change in drag was considerable. This was the result of increased compression of the flow on the aft portion of the boattail at higher Reynolds numbers. The cause of this phenomenon appeared to be a decrease in the amount of separated flow on the aft boattail surface.

Data were taken at altitudes between 3048 and 16 764 meters (10 000 and 55 000 ft) and Reynolds numbers between 70.0×10^6 and 16.0×10^6. Angle of attack was varied from 2.4° to 9.4°, and Mach number varied from 0.6 to 0.975.

SYMBOLS

A	area
A_{E8}	nozzle effective throat area (hot), cm^2; $in.^2$
A_e	nozzle exit area, 903.07 cm^2; 139.98 $in.^2$
A_{max}	maximum cross-sectional area, 3167.12 cm^2; 490.87 $in.^2$
C_D	drag coefficient, D/q_0A_{max}
C_p	pressure coefficient, $p - p_0/q_0$
D	pressure drag, N; lb
h	altitude, m; ft
L	characteristic length, 5.18 m; 1700 ft
l	nozzle length, 61.47 cm; 24.20 in.
M	Mach number
P	total pressure, N/m^2; psia
p	static pressure, N/m^2; psia

q dynamic pressure, N/m^2; psia

Re Reynolds number, $\rho vL/\mu$

T total temperature, K; ^{o}R

v velocity, m/sec; ft/sec

x axial distance from boattail shoulder nacelle station at 530.63 cm (208.91 in.)

y radial distance from nozzle centerline to boattail surface, cm; in.

α angle of attack, deg

μ coefficient of viscosity, $(N)(sec)/m^2$; slugs/(ft)(sec)

ρ density, kg/m^3; $slugs/ft^3$

Subscripts:

B boattail

0 free stream

8 primary nozzle throat station

APPARATUS AND PROCEDURE

Installation

Details of the airplane modifications and the nacelle-engine assembly are given in references 2 and 3. A schematic and a photograph of the nacelle and boattail nozzle are shown in figures 2 and 3. The nacelle was located at the 32 percent semispan and alined parallel to the aircraft centerline. The nacelle had a downward incidence of $4\frac{1}{2}^{o}$ (relative to the wing chord) so that the aft portion of the nacelle was tangent to the aft wing lower surface, and the clearance at the wing trailing edge was approximately 0.64 centimeter (0.25 in.). Details of the wing modifications, nacelle shape, and mounting strut are given in reference 3. The strut with the wide fairing described in reference 3 was used.

The gas generator for this nozzle was a J85-GE-13 turbojet engine with an afterburner. The variable-area primary nozzle was locked at 709.70 square centimeters (110.00 $in.^2$) and permitted operation at military or part power. The secondary cooling airflow was controlled by a rotary valve just ahead of the compressor (fig. 2). Because the ratio of the nozzle exit area to primary area was small ($A_e/A_8 = 1.28$), this nozzle could pump only small amounts of secondary air (approximately 1 percent of the primary flow); so the secondary flow valve was fixed in the full-open position.

Test Hardware

A photograph of the boattail installed on the aircraft is shown in figure 4. The dimensions of the nozzle and boattail are shown in figure 5. The boattail had local boattail angles as high as 31°. The ratio of nozzle exit area to nacelle area A_e/A_{max} was 0.29. The coordinates of the contoured boattail are also listed in figure 5. A nickel-chromium base alloy (rolled alloy 333) was used for the internal portions of the nozzle, and the external parts were predominately 304 stainless steel.

Instrumentation

A new data recording system was developed specifically for the F-106 program (ref. 4), and as a result it was possible to instrument the nozzle quite extensively (see fig. 6). The nozzle had 12 rows of static-pressure orifices equally spaced circumferentially around the boattail. There were nine ports in each row spanning the length of the boattail, and all 108 pressure taps were area weighted to simplify the boattail drag calculations. Thirteen static-pressure orifices were located on the cylindrical section upstream of the boattail.

Tufts were mounted on the upper quadrant of the boattail, and pictures of the tufts were taken with a high-speed motion-picture camera mounted in the tail (see ref. 5). The camera was integrated with the data system so that it ran only during each of the 11.60-second data scan periods.

Procedure

All the flights were made from Selfridge Air National Guard Base in Mt. Clemens, Michigan, in a test corridor over Lake Huron. A total of three flights were made and the majority of the data were taken at Mach numbers of 0.7 and 0.9. The ranges of flight variables, speed, altitude, angle of attack, and load factor, are listed in table I. The majority of the data were taken in coordinated turns. The means of varying the Reynolds number was to change altitude while holding the Mach number constant. By flying in turns, angle of attack as well as Mach number could be held constant. Also, at a given altitude and Mach number, angle of attack could be varied by flying tighter turns and increasing the load factor. The data points for Mach number variation were taken in level flight. The lowest Reynolds number data point was taken in a pushover maneuver. This data point was taken at an altitude of 16 764 meters (55 000 ft), where the F-106B will not fly straight and level at a Mach number of 0.9. The J-85 engine was run at

military power for all of the data points, and the nominal nozzle pressure ratios were 3.2 at Mach 0.7 and 3.9 at Mach 0.9.

Data Reduction

Engine airflow was determined by using prior engine calibration data (ref. 7) along with in-flight measurements of engine speed, pressure, and temperature at the compressor face. With the compressor inlet flow, the total pressure and temperature at the turbine discharge, and the fuel flow rates known, other parameters at the primary nozzle exit, such as effective area A_{E8}, total pressure P_8, and total temperature T_8, were obtained from previous calibrations. All the drag values were determined by pressure integration.

The accuracy of the pressure data recorded on this test was improved somewhat over that on previous tests (ref. 5). This improvement was primarily due to more timely and exacting calibrations of the Scanivalve transducers. All of the transducers had one port measuring a common pressure, the nose boom free-stream static pressure. These values, for each data point, measured on the transducers were averaged. All the pressures on any one transducer were then adjusted by the difference between the average value and the value measured by that transducer. This procedure accounted for slight differences in calibrations or small shifts in calibration from one data point to the next.

The data recorded on the lowest Reynolds number point are open to some question. These data were taken in a pushover maneuver, and the altitude was changing during the data scan, in particular at the end of the data scan. The pressures measured at the end of the data scan showed a definite shift that could be correlated with an altitude loss. Pressures from other data points where altitude was stable, and data recorded early in this data scan were used to adjust the values shifted by the altitude change. These adjustments resulted in a shift in drag coefficient of only 0.007. The data presented were corrected by this amount.

RESULTS AND DISCUSSION

Reynolds Number

On previous tests of other boattail geometries (refs. 5 and 6) Reynolds number had a very significant effect on boattail drag. On this boattail, Reynolds number also produced an effect on boattail drag, but it was considerably less than on most other geometries. The range of Reynolds number was approximately 16.0×10^6 to 70.0×10^6.

The Reynolds number was based on a characteristic length of 5.18 meters (17.00 ft), which took into consideration the wing chord at this station (approximately 7.32 m; 24.00 ft) and the nacelle length (approximately 3.96 m; 13.00 ft).

Tests were run over ranges of Reynolds number at Mach numbers of 0.7 and 0.9. The data at Mach 0.9 are presented in two portions at different angles of attack. The boattail drag results at the lower angle of attack (2.4° to 4.6°) are shown in figure 7. The effect of Reynolds number in this range was small. The drag decreased only slightly with increasing Reynolds number. The cause for this change in drag can be clearly seen in the pressure profiles in figure 8. The vertical scale in this figure has been expanded in order to emphasize the small differences in the pressures on the aft boattail. This expanded scale also emphasizes the improved accuracy that was obtained in this test over that in the previous ones (ref. 5).

The change in drag with Reynolds number resulted from increasing compression of the flow on the aft portion of the boattail. These changes occurred even though the flow was separated over a large portion of the boattail. Tufts were mounted on the upper quadrant of the boattail, and high-speed motion pictures were taken with a camera in the tail of the F-106. Only small changes in the tufts were noticeable between high and low Reynolds numbers, but at all conditions there was a very obvious separated flow over the rear half of the boattail. This is shown in figure 9. A small change in the separation point could have resulted in these changes in the pressures.

As the Reynolds number is increased, the boundary layer becomes thinner. With a thinner boundary layer the flow in it has more energy and can traverse an adverse pressure gradient farther before separating. This effect results in more compression and higher pressures on the boattail. On this boattail, with its very high local boattail angles, the separation point was almost fixed. Changes in boundary-layer thickness could not affect the separation point as on other boattails (refs. 5 and 6), and so only minimal changes in separation, pressures, and drag were seen.

The drag data at the higher angle of attack (5.5° to 7.8°) at Mach 0.9 are shown in figure 10. At high angles of attack it was possible to test at lower Reynolds numbers because the aircraft could be flown at higher altitudes. The lowest Reynolds number data point (16.0×10^6) was taken in a pushover maneuver at an altitude of 16 764 meters (55 000 ft). The pushover maneuver did create some problems, as discussed in the section Data Reduction. At the higher Reynolds numbers, above 35.0×10^6, the effect of Reynolds number on boattail drag was small. However, at lower values, below 35.0×10^6, the effect increased. The pressure profiles in figure 11 show that pressures dropped off with decreasing Reynolds number, which indicates the separation point was moving upstream. Figure 12 shows changes in tuft positions which, although small, also indicate the separation was moving upstream.

Some of the pressure profiles, in particular those at the high Reynolds numbers, may not appear to represent a separated flow. They do not only because of the expanded

scale used to show the differences that resulted on the aft boattail. If the scale were changed, the pressure curves would look quite different. Figure 13 shows the same pressures without the expanded scale and plotted against percent of boattail projected area. In this figure all the pressures indicate a separated flow over a majority of the boattail area. This figure also explains why the drag of this boattail was much lower than might be expected. First, because of the gradual turn at the shoulder the flow never expanded to an extremely low pressure as on other geometries. Second, the geometry was such that the flow began recompressing quickly, and therefore the region where the low pressures did exist covered only a small portion of the total projected aft-facing area. Third, because the flow recompressed quickly before separating, the pressures were high in the region of separated flow and it had almost no net force. The end result was a low drag.

Figure 14 shows the effect of Reynolds number on boattail drag at a Mach number of 0.7. A change in Reynolds number of the same magnitude was achieved at Mach 0.7 as at Mach 0.9. The effects at Mach 0.7 were similar to those at Mach 0.9, but this geometry seems to have been more sensitive to Reynolds number at the lower Mach number. The corresponding pressure profiles are shown in figure 15. As before there was an increase in compression on the aft boattail with increasing Reynolds number.

Mach Number

The effect of Mach number on boattail drag is shown in figure 16. As the Mach number was increased, a terminal shock was formed on the wing and began moving aft. At a Mach number near 0.95 the shock moved off the back of the nacelle, and the result was a drastic increase in boattail drag. This effect was common to all nozzles tested in this installation and is further explained in reference 3.

Angle of Attack

The effect of angle of attack on boattail drag at both Mach numbers of 0.7 and 0.9 is shown in figure 17. At Mach 0.7 there was little or no effect of angle of attack on boattail drag. At Mach 0.9 there was a slight increase in drag with increasing angle of attack.

SUMMARY OF RESULTS

A scaled version of a boattail nozzle typical of those used on a twin-engine fighter aircraft was installed just below and aft of the wing trailing edge on an F-106B aircraft and was tested at subsonic speeds. The nozzle was fixed in the closed, or military power, configuration. The effects on boattail drag of Reynolds number, angle of attack, and Mach number were investigated. The following results were obtained:

1. Increasing the Reynolds number, by reducing altitude (changing density and viscosity), resulted in a slight decrease in boattail drag at both Mach numbers of 0.7 and 0.9.

2. Increasing the Reynolds number produced a modest increase in compression of the flow on the aft boattail, even though the flow was separated over approximately 50 percent of the projected boattail area at both high and low Reynolds numbers.

3. This boattail nozzle had relatively low drag even though the flow was separated over a major portion of the aft-facing boattail area.

4. At Mach 0.7 no effect of angle of attack was detected, but at Mach 0.9 there was a slight increase in boattail drag with increasing angle of attack.

Lewis Research Center,
National Aeronautics and Space Administration,
Cleveland, Ohio, January 14, 1974,
501-24.

REFERENCES

1. Wilcox, Fred A.; Samanich, Nick E.; and Blaha, Bernard J.: Flight and Wind Tunnel Investigation of Installation Effects on Supersonic Cruise Exhaust Nozzles at Transonic Speeds. Paper 69-427, AIAA, June 1969.

2. Crabs, Clifford C.: An Inflight Investigation of Airframe Effects on Propulsion System Performance at Transonic Speeds. Soc. of Experimental Test Pilots, Technical Review, vol. 9, no. 4, 1969, pp. 51-66.

3. Mikkelson, Daniel C.; and Head, Verlon L.: Flight Investigation of Airframe Installation Effects on a Variable Flap Ejector Nozzle of an Underwing Engine Nacelle at Mach Numbers from 0.5 to 1.3. NASA TM X-2010, 1970.

4. Groth, Harold W.; Samanich, Nick E.; and Blumenthal, Philip Z.: Inflight Thrust Measuring System for Underwing Nacelles Installed on a Modified F-106 Aircraft. NASA TM X-2356, 1971.

5. Chamberlin, Roger: Flight Investigation of 24^{o} Boattail Nozzle Drag at Varying Subsonic Flight Conditions. NASA TM X-2626, Nov. 1972.

6. Chamberlin, Roger; and Blaha, Bernard J.: Flight and Wind Tunnel Investigation of the Effects of Reynolds Number on Installed Boattail Drag at Subsonic Speeds. Paper 73-139, AIAA, Jan. 1973.

7. Antl, Robert J.; and Burley, Richard R.: Steady-State Airflow and Afterburning Performance Characteristics of Four J85-GE-13 Turbojet Engines. NASA TM X-1742, 1969.

TABLE I. - FLIGHT TEST VARIABLES

Altitude, h		Flight Mach number, M_0					
m	ft	0.7			0.9		
		Target angle of attack, α, deg	Nominal Reynolds number, Re	Load factor	Target angle of attack, α, deg	Nominal Reynolds number, Re	Load factor
3 048	10 000	7	64.1×10^6	2.3	-------	--------	---------
4 572	15 000	7, 9	55.3	1.9, 2.5	5	71.0×10^6	2.3
6 096	20 000	5 to 11	47.3	1.1 to 2.6	5	60.8	1.9
7 620	25 000	7, 9	40.4	1.2, 1.6	5, 8	51.9	1.5, 2.6
[a]9 144	30 000	7, 9	34.2	1.0, 1.3	5, 8	43.9	1.2, 2.1
10 668	35 000	9	28.7	1.1	5.5 to 9	36.9	1.1 to 1.9
12 192	40 000	------	--------	---------	8	29.4	1.3
13 716	45 000	------	--------	---------	8	23.1	1.0
16 764	55 000	------	--------	---------	8	14.3	[b]<1.0

[a]Mach number variation in level flight, 0.6, 0.65, 0.70, 0.75, 0.80, 0.85, 0.90, 0.975.
[b]Pushover maneuver.

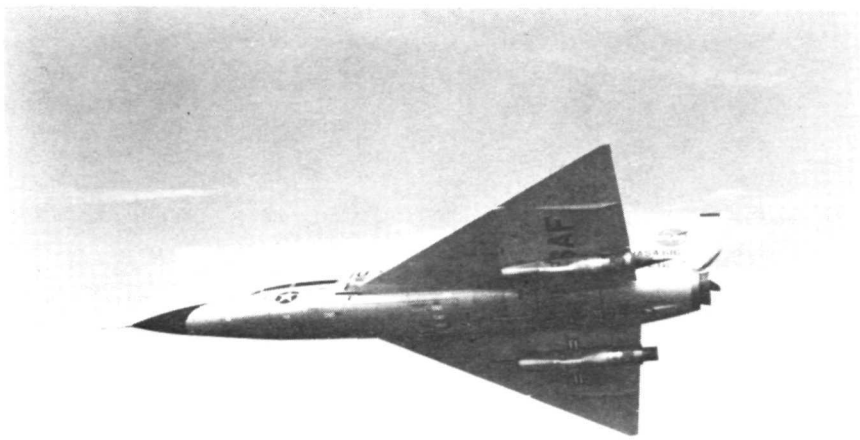

C-69-2871

Figure 1. - Modified F-106B inflight.

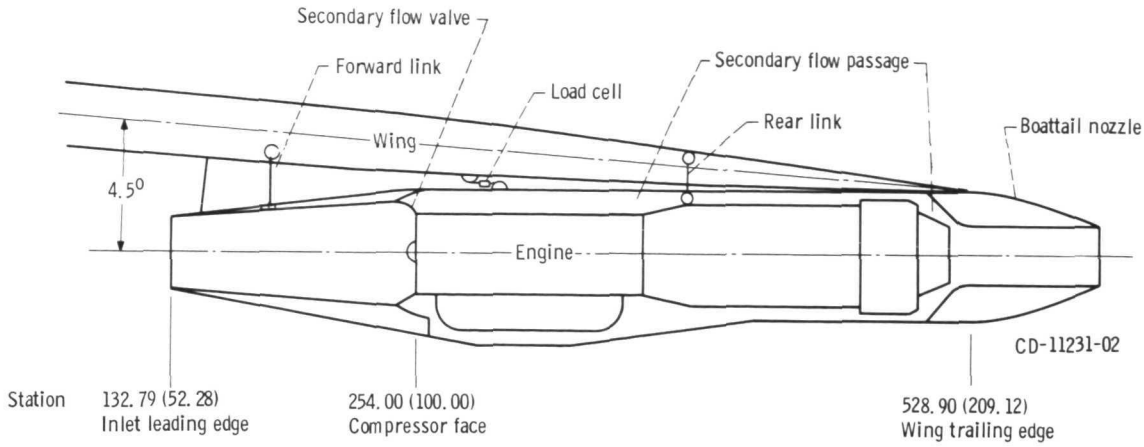

Figure 2. - Schematic of nozzle installation. (Dimensions in centimeters (in.).)

Figure 3. - Nacelle installation.

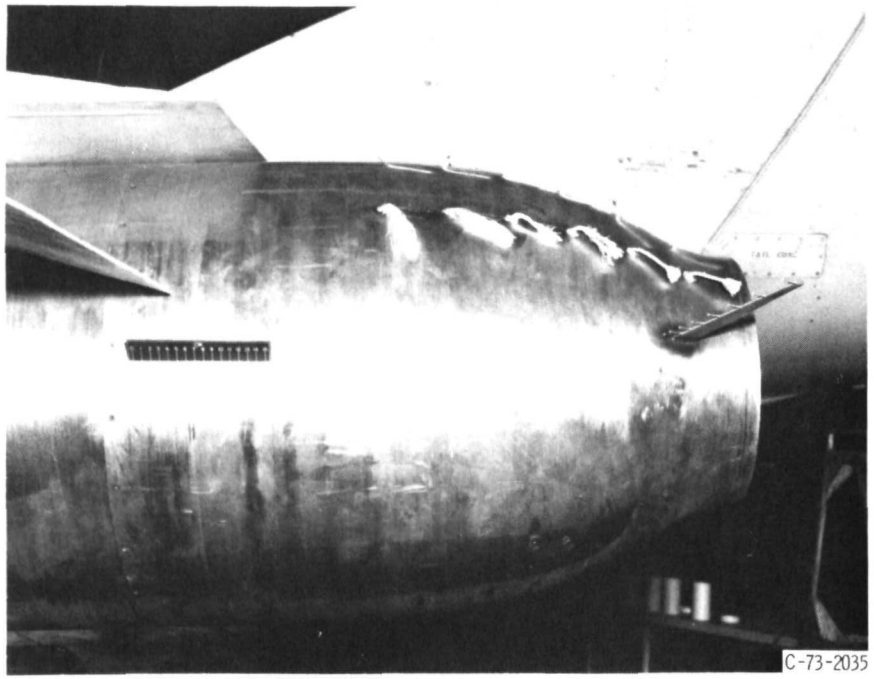

Figure 4. - Contoured boattail - cruise configuration.

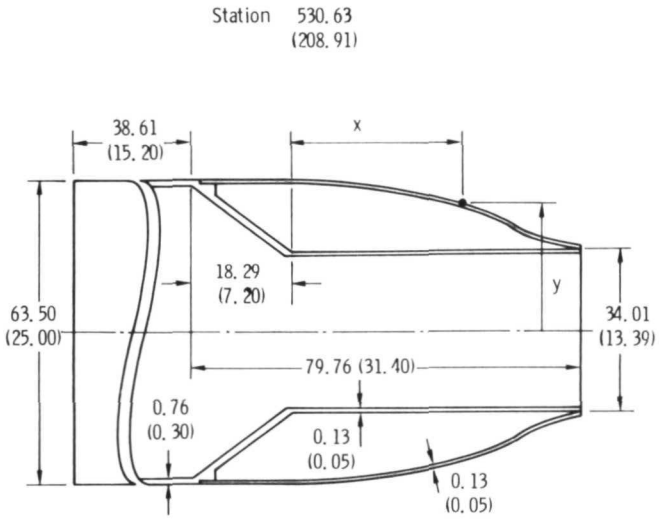

x		y	
cm	in.	cm	in.
0	0	31.75	12.50
5.08	2.00	31.67	12.47
10.16	4.00	31.55	12.42
15.24	6.00	31.37	12.35
20.32	8.00	30.91	12.17
25.40	10.00	30.15	11.87
30.48	12.00	29.29	11.53
35.56	14.00	27.89	10.98
40.64	16.00	25.98	10.23
45.72	18.00	23.62	9.30
50.80	20.00	20.83	8.20
53.34	21.00	19.30	7.60
55.88	22.00	18.29	7.20
58.42	23.00	17.55	6.91
60.33	23.75	17.27	6.80

Figure 5. - Boattail nozzle dimensions. (Dimensions in centimeters (in.).)

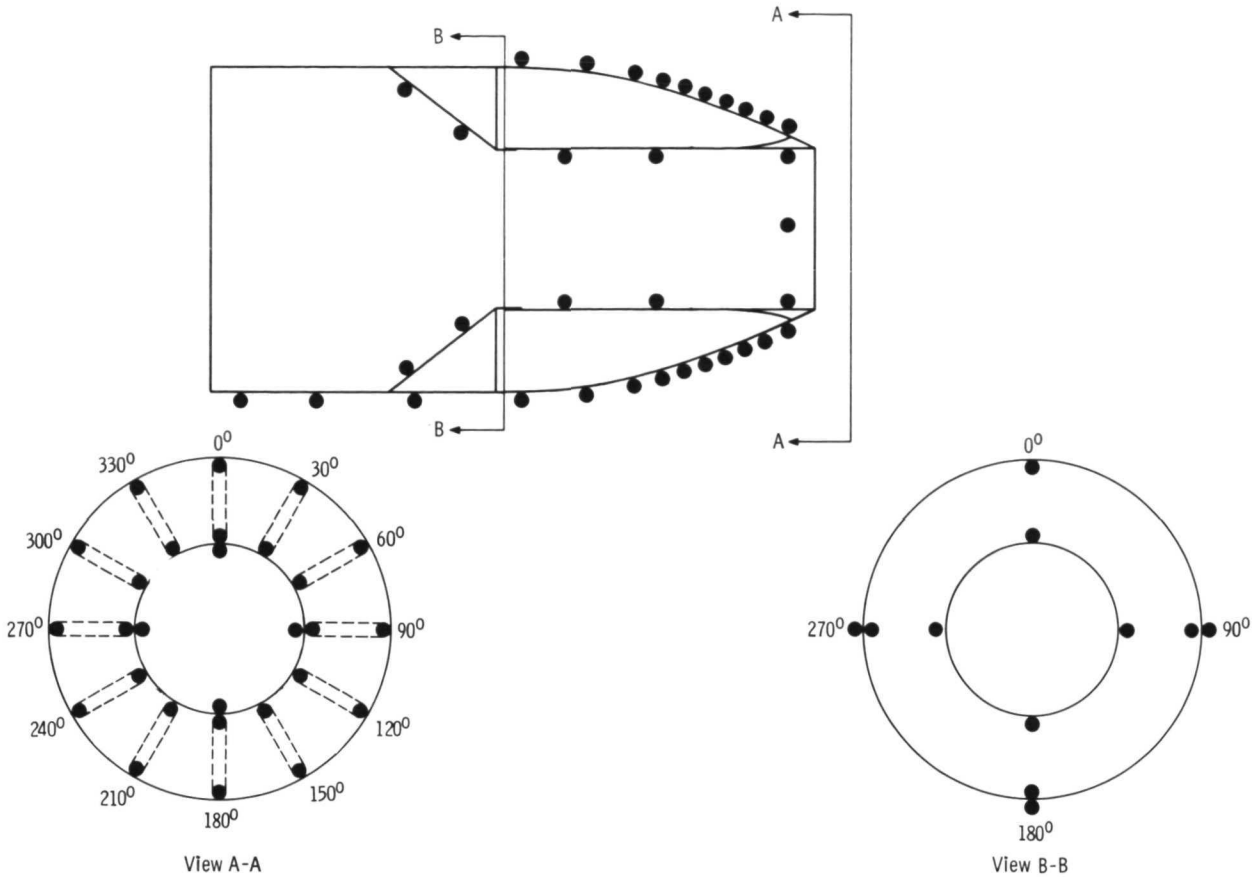

Figure 6. - Boattail nozzle static-pressure instrumentation.

CD-11233-02

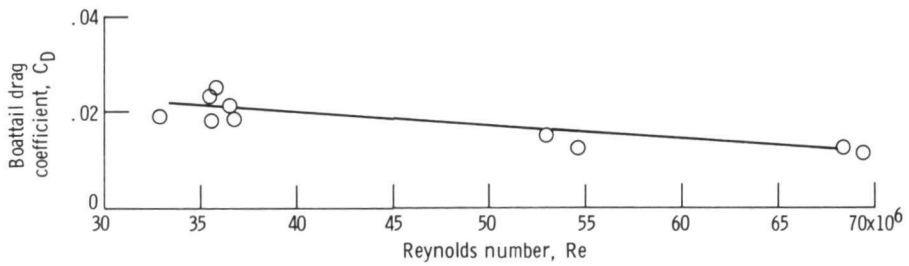

Figure 7. - Reynolds number effect on boattail drag coefficient. Mach number, 0.9; angle of attack, 2.4° to 4.6°; characteristic length, 5.18 meters (17.00 ft).

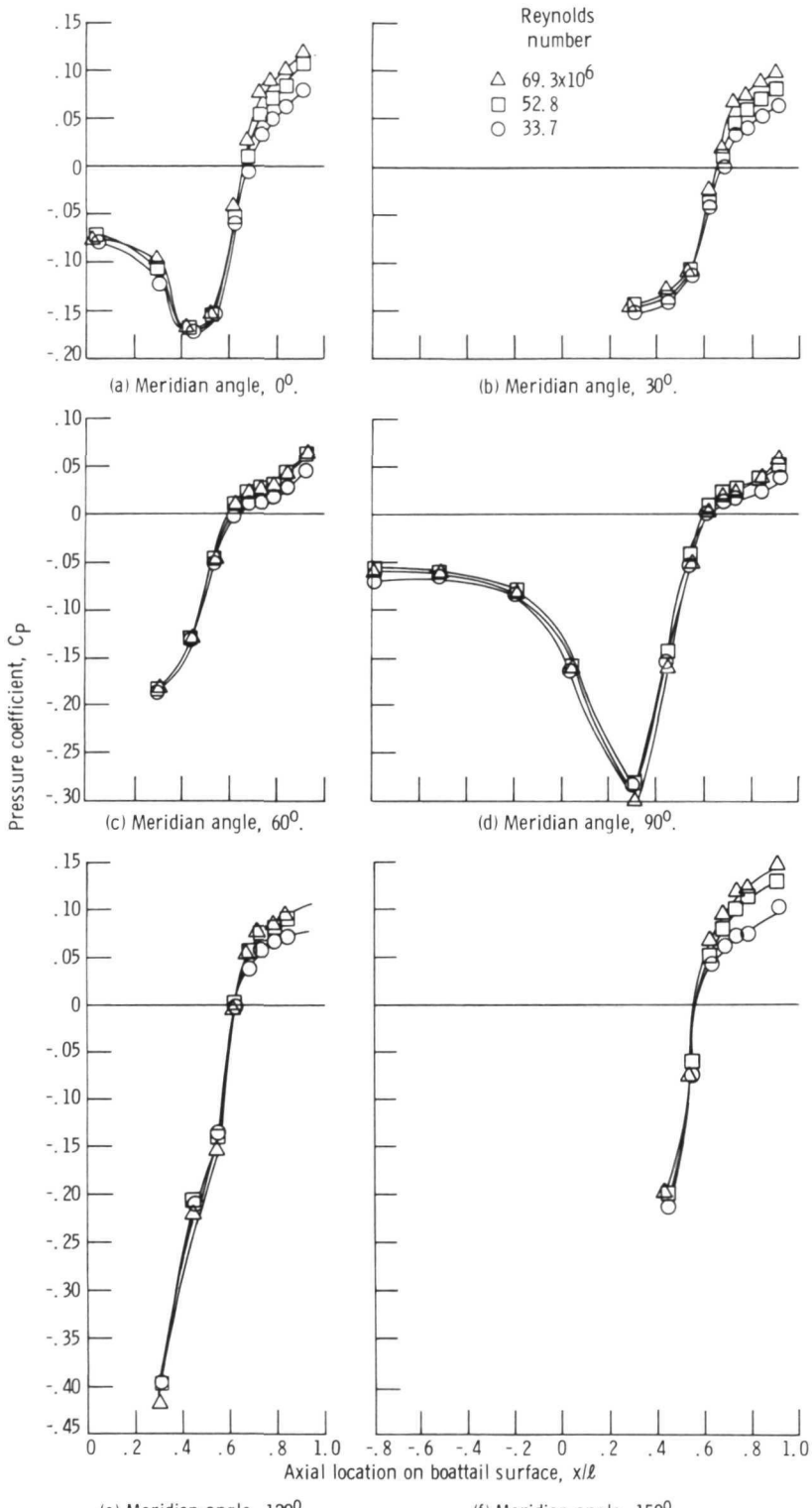

Figure 8. - Effect of Reynolds number on boattail pressure distribution. Mach number, 0.9; angle of attack, 2.9° to 4.6°.

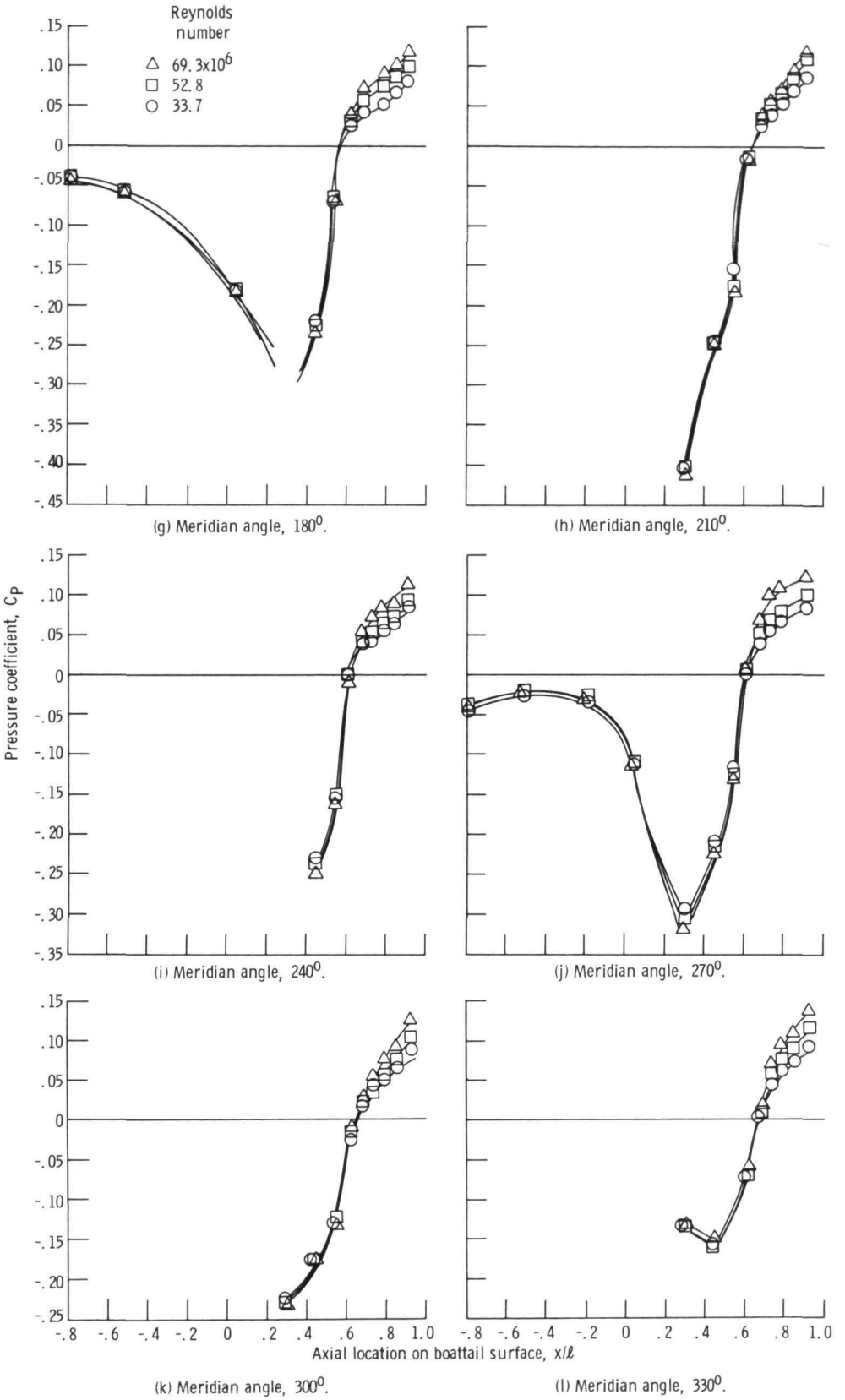

(g) Meridian angle, 180°.

(h) Meridian angle, 210°.

(i) Meridian angle, 240°.

(j) Meridian angle, 270°.

(k) Meridian angle, 300°.

(l) Meridian angle, 330°.

Figure 8. - Concluded.

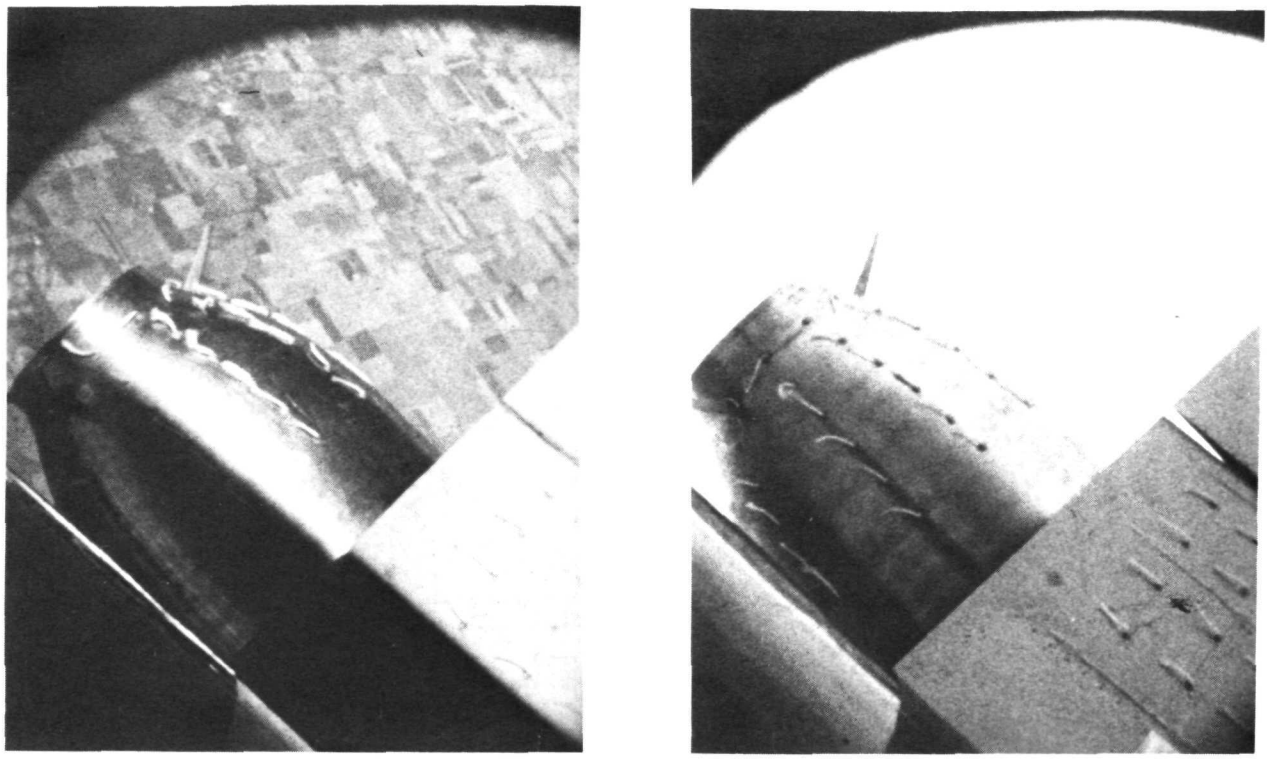

(a) Reynolds number, 35.7×10^6.

(b) Reynolds number, 69.4×10^6.

Figure 9. - Tuft patterns at high and low Reynolds numbers. Mach number, 0.9; angle of attack, 2.4° to 4.6°.

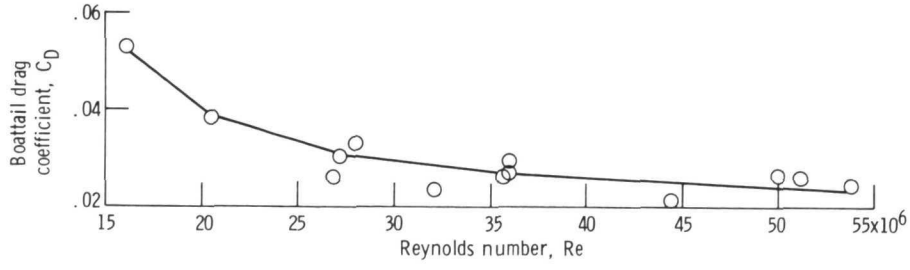

Figure 10. - Reynolds number effect on boattail drag coefficient. Mach number, 0.9; angle of attack, 5.5^0 to 7.8^0; characteristic length, 5.18 meters (17.00 ft).

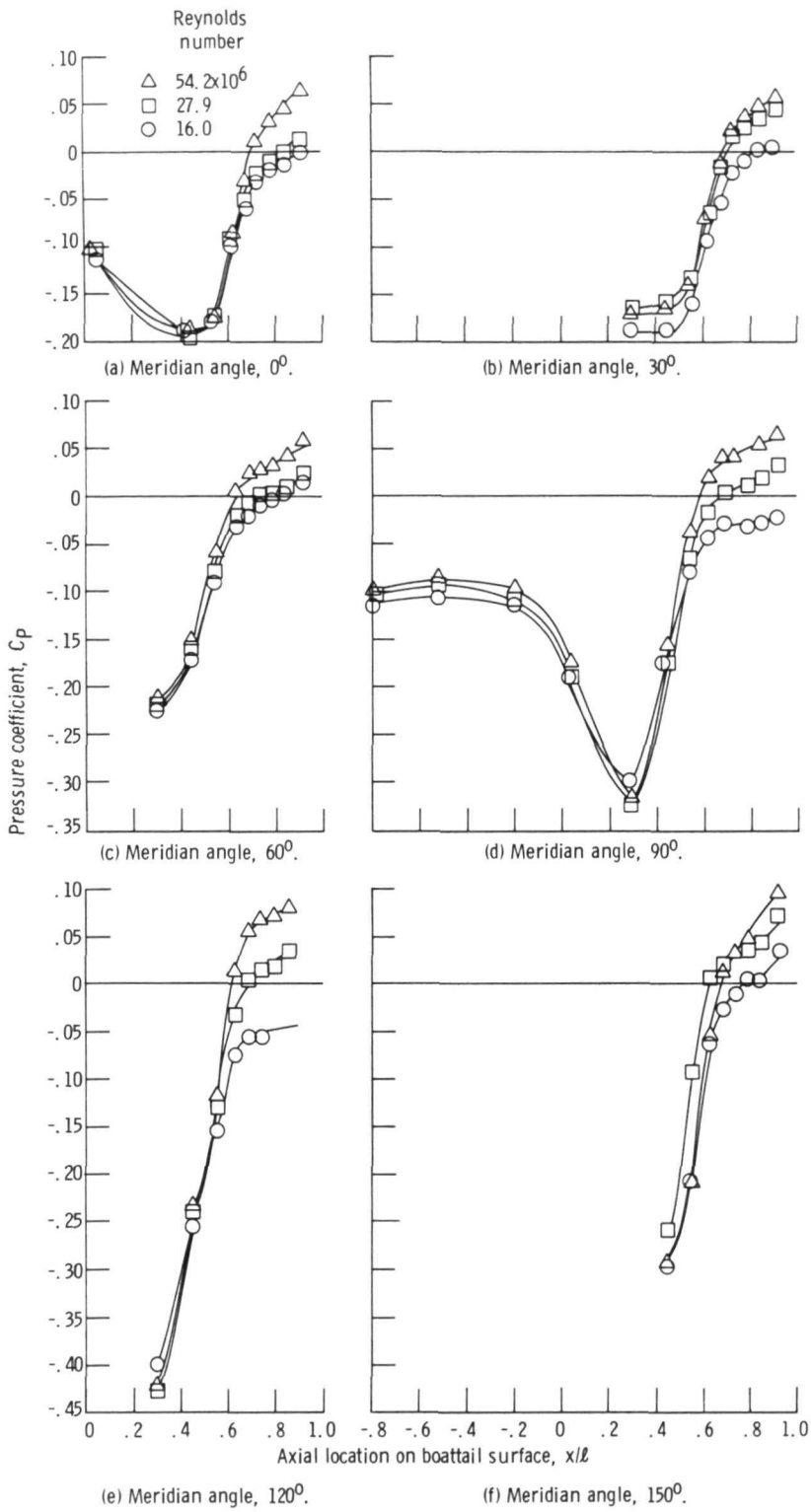

Figure 11. - Effect of Reynolds number on boattail pressure distribution. Mach number, 0.9; angle of attack, 5.5° to 7.8°.

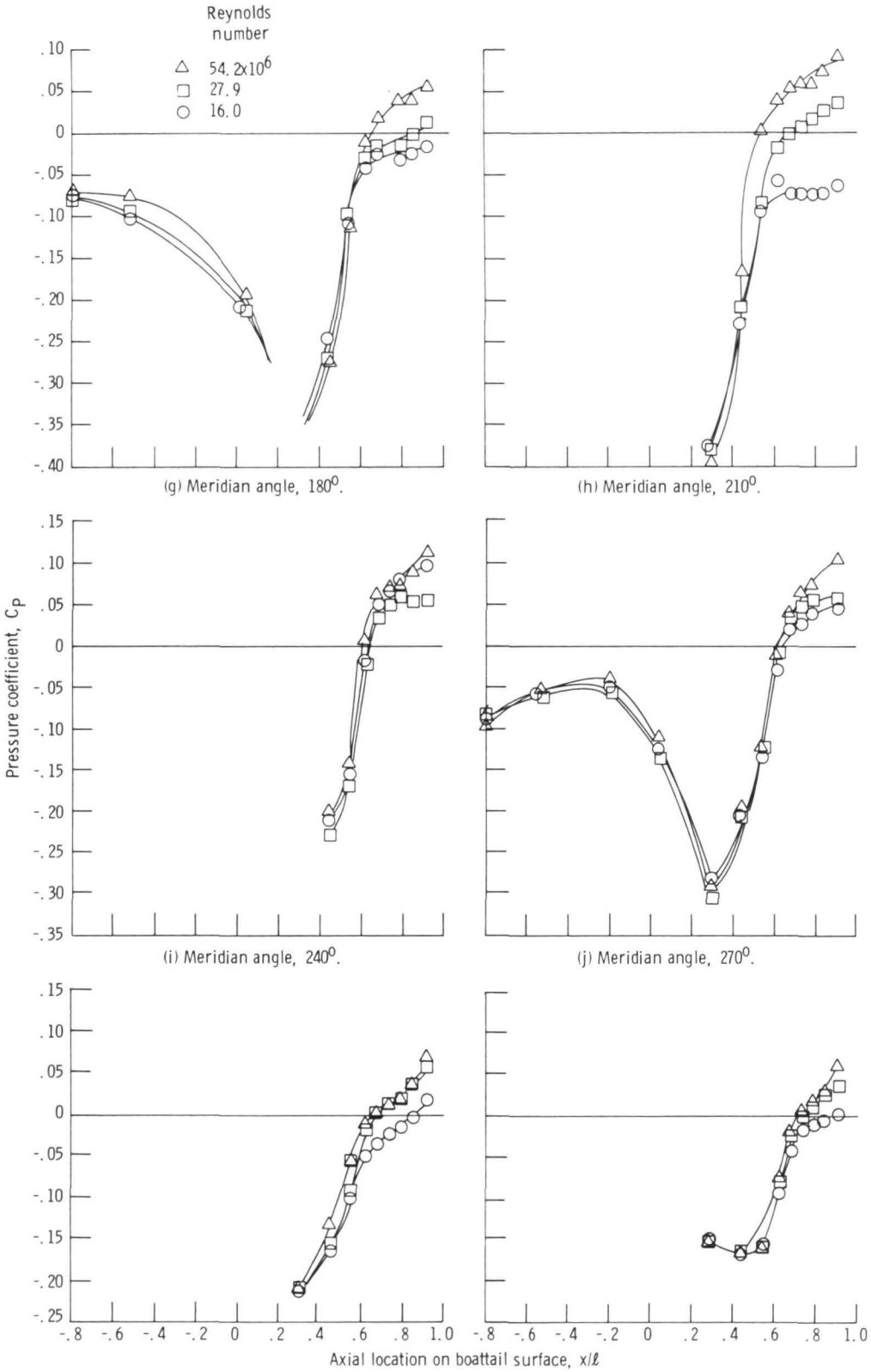

(g) Meridian angle, 180°.

(h) Meridian angle, 210°.

(i) Meridian angle, 240°.

(j) Meridian angle, 270°.

(k) Meridian angle, 300°.

(l) Meridian angle, 330°.

Figure 11. - Concluded.

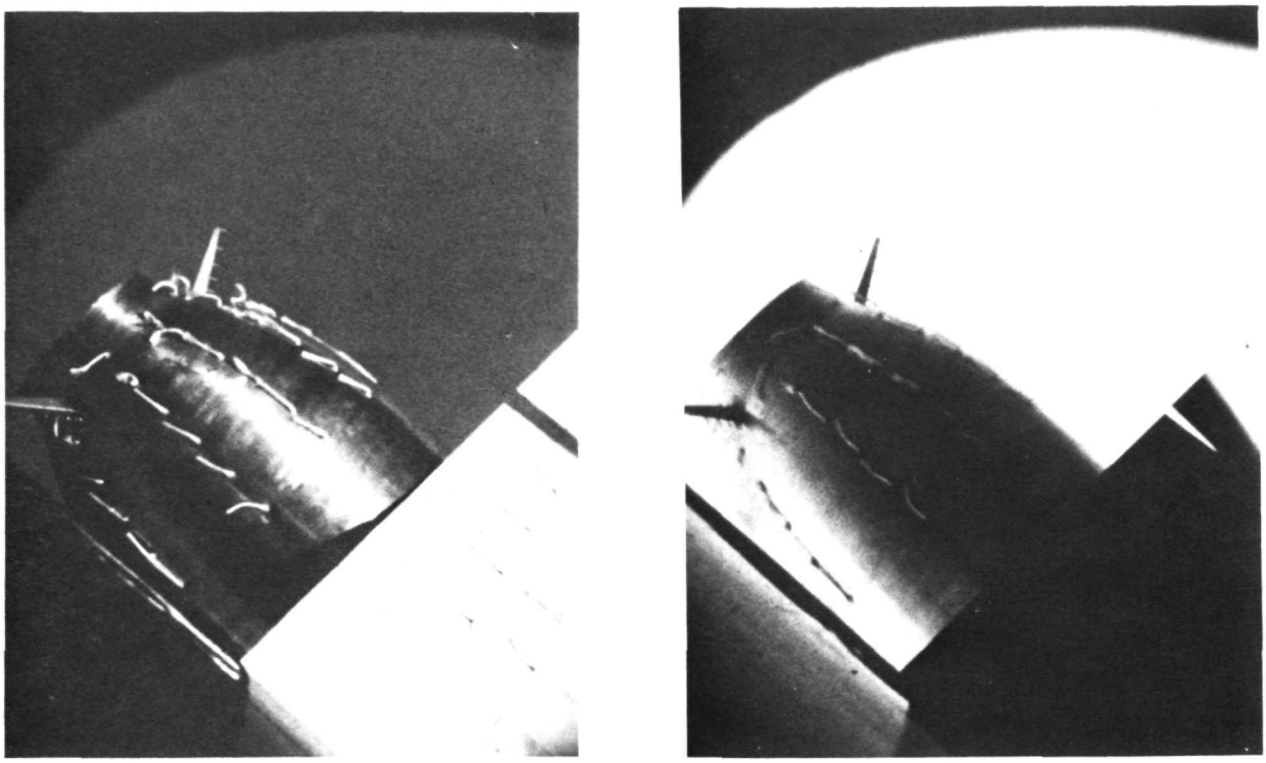

(a) Reynolds number, 16.0×10^6.

(b) Reynolds number, 44.3×10^6.

Figure 12. - Tuft patterns at high and low Reynolds numbers. Mach number, 0.9; angle of attack, 5.5° to 7.8°.

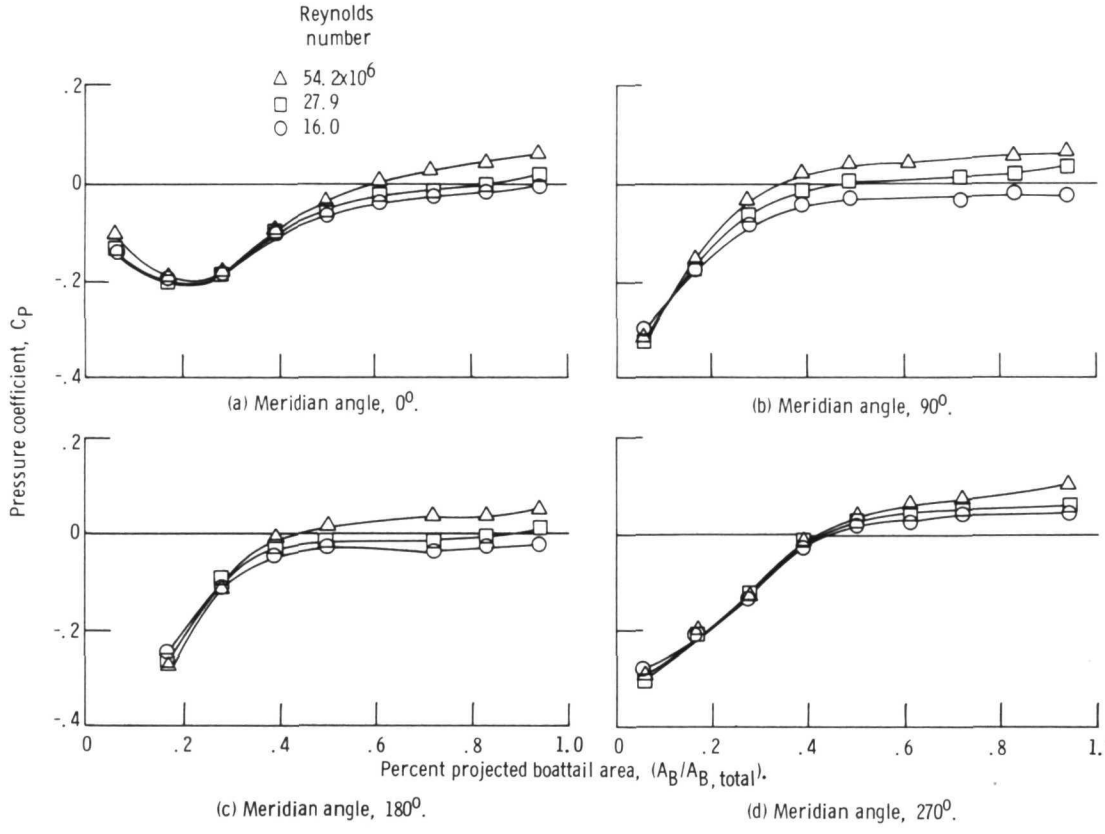

Figure 13. - Boattail pressures on increments of equal projected area Mach number, 0.9; angle of attack, 5.5° to 7.8°.

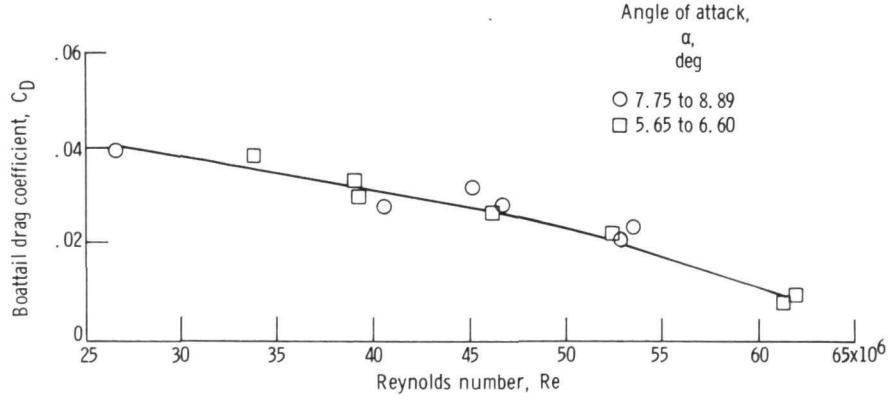

Figure 14. - Reynolds number effect on boattail drag coefficient. Mach number, 0.7; characteristic length, 5.18 meters (17.00 ft).

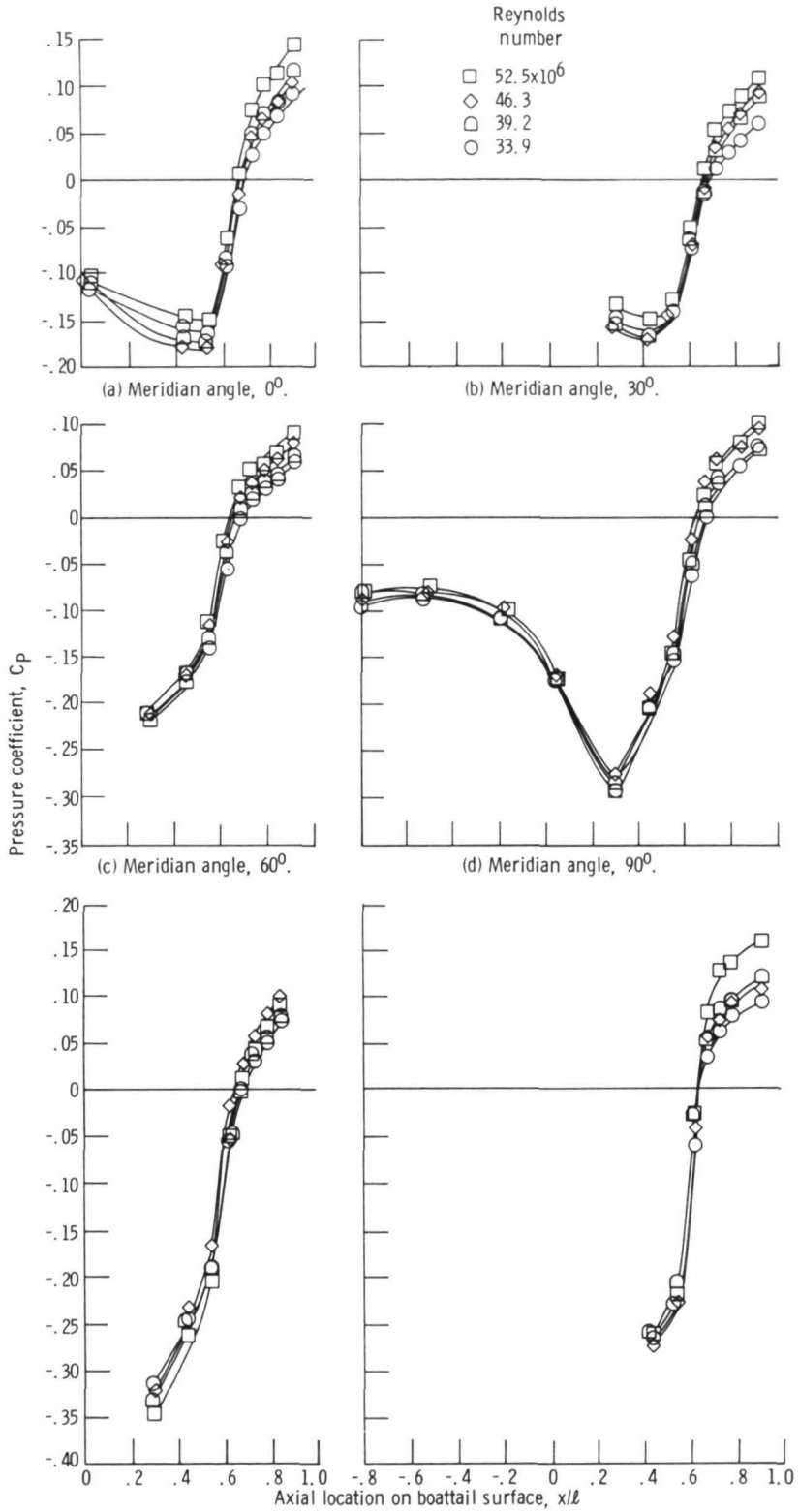

Figure 15. - Effect of Reynolds number on boattail pressure distribution. Mach number, 0.7; angle of attack, 5.6° to 8.9°.

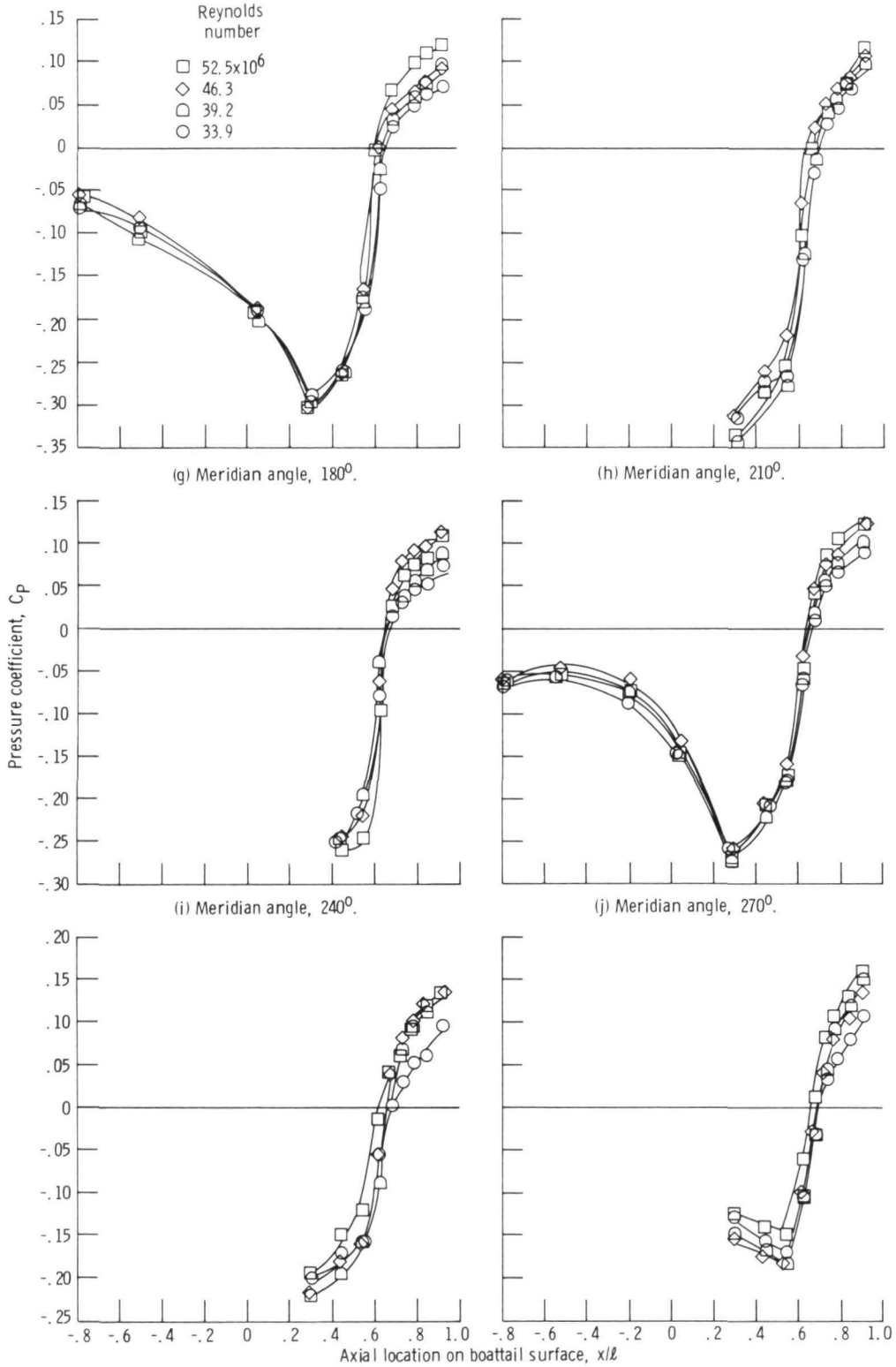

(g) Meridian angle, 180°.

(h) Meridian angle, 210°.

(i) Meridian angle, 240°.

(j) Meridian angle, 270°.

(k) Meridian angle, 300°.

(l) Meridian angle, 330°.

Figure 15. - Concluded.

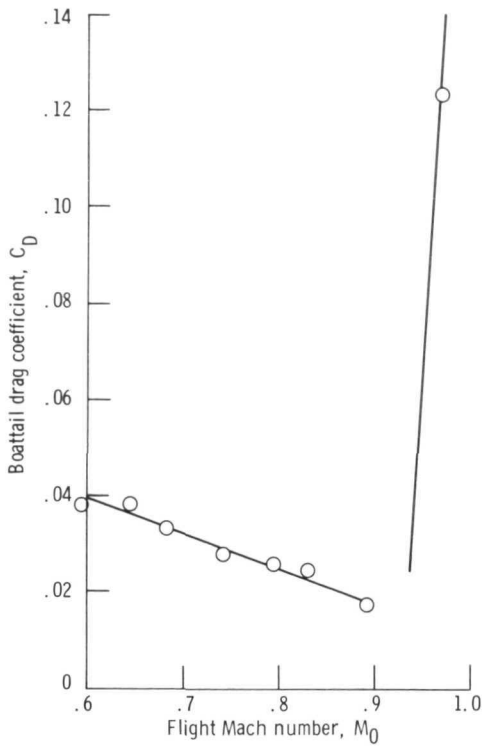

Figure 16. - Mach number effect on boattail drag. Level flight; altitude, 7620 meters (25 000 ft).

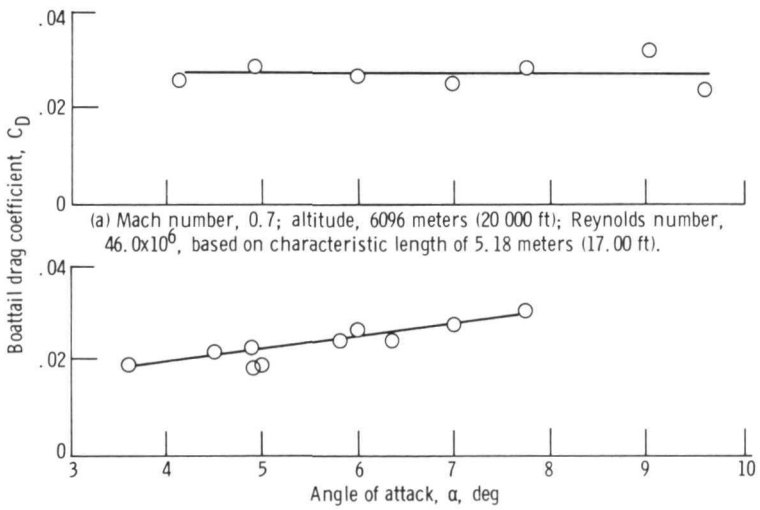

(a) Mach number, 0.7; altitude, 6096 meters (20 000 ft); Reynolds number, 46.0×10^6, based on characteristic length of 5.18 meters (17.00 ft).

(b) Mach number, 0.9; altitude, 10 668 meters (35 000 ft); Reynolds number, 35.0×10^6, based on characteristic length of 5.18 meters (17.00 ft).

Figure 17. - Angle of attack effect on boattail drag coefficient.

NATIONAL AERONAUTICS AND SPACE ADMINISTRATION
WASHINGTON, D.C. 20546

OFFICIAL BUSINESS
PENALTY FOR PRIVATE USE $300

SPECIAL FOURTH-CLASS RATE
BOOK

POSTAGE AND FEES PAID
NATIONAL AERONAUTICS AND
SPACE ADMINISTRATION
451

U.S.MAIL

POSTMASTER: If Undeliverable (Section 158 Postal Manual) Do Not Return

"The aeronautical and space activities of the United States shall be conducted so as to contribute . . . to the expansion of human knowledge of phenomena in the atmosphere and space. The Administration shall provide for the widest practicable and appropriate dissemination of information concerning its activities and the results thereof."

—NATIONAL AERONAUTICS AND SPACE ACT OF 1958

NASA SCIENTIFIC AND TECHNICAL PUBLICATIONS

TECHNICAL REPORTS: Scientific and technical information considered important, complete, and a lasting contribution to existing knowledge.

TECHNICAL NOTES: Information less broad in scope but nevertheless of importance as a contribution to existing knowledge.

TECHNICAL MEMORANDUMS: Information receiving limited distribution because of preliminary data, security classification, or other reasons. Also includes conference proceedings with either limited or unlimited distribution.

CONTRACTOR REPORTS: Scientific and technical information generated under a NASA contract or grant and considered an important contribution to existing knowledge.

TECHNICAL TRANSLATIONS: Information published in a foreign language considered to merit NASA distribution in English.

SPECIAL PUBLICATIONS: Information derived from or of value to NASA activities. Publications include final reports of major projects, monographs, data compilations, handbooks, sourcebooks, and special bibliographies.

TECHNOLOGY UTILIZATION PUBLICATIONS: Information on technology used by NASA that may be of particular interest in commercial and other non-aerospace applications. Publications include Tech Briefs, Technology Utilization Reports and Technology Surveys.

Details on the availability of these publications may be obtained from:

SCIENTIFIC AND TECHNICAL INFORMATION OFFICE

NATIONAL AERONAUTICS AND SPACE ADMINISTRATION

Washington, D.C. 20546